HHS Public Access

Author manuscript

Nat Med. Author manuscript; available in PMC 2017 July 17.

Published in final edited form as:

Nat Med. 2017 January ; 23(1): 128–135. doi:10.1038/nm.4244.

Interleukin-33-induced expression of PIBF1 by decidual B cells protects against preterm labor

Bihui Huang[1,14], **Azure N Faucette**[1,13,14], **Michael D Pawlitz**[1], **Bo Pei**[1], **Joshua W Goyert**[1], **Jordan Zheng Zhou**[1], **Nadim G El-Hage**[1], **Jie Deng**[2], **Jason Lin**[1], **Fayi Yao**[1], **Robert S Dewar III**[1], **Japnam S Jassal**[1], **Maxwell L Sandberg**[3], **Jing Dai**[1], **Montserrat Cols**[4], **Cong Shen**[4], **Lisa A Polin**[5], **Ronald A Nichols**[1,6], **Theodore B Jones**[1,6], **Martin H Bluth**[7], **Karoline S Puder**[1], **Bernard Gonik**[1], **Nihar R Nayak**[1], **Elizabeth Puscheck**[1], **Wei-Zen Wei**[5], **Andrea Cerutti**[8,9,10,11], **Marco Colonna**[11,12], and **Kang Chen**[1,5,11]

[1]Department of Obstetrics and Gynecology, Wayne State University, Detroit, Michigan, USA

[2]Department of Obstetrics, Gynecology and Reproductive Sciences, Yale School of Medicine, New Haven, Connecticut, USA

[3]Leadership in Medicine Program, Union College, Schenectady, New York, USA

[4]Immunology Program, Memorial Sloan Kettering Cancer Center, New York, New York, USA

[5]Department of Oncology, Wayne State University, Detroit, Michigan, USA

[6]Department of Obstetrics and Gynecology-Med Ed, Beaumont Dearborn Hospital, Dearborn, Michigan, USA

[7]Department of Pathology, Wayne State University, Detroit, Michigan, USA

[8]Catalan Institute for Research and Advanced Studies, Barcelona Biomedical Research Park, Barcelona, Spain

[9]Program for Inflammatory and Cardiovascular Disorders, Institut Hospital del Mar d'Investigacions Mèdiques, Barcelona, Spain

[10]Immunology Institute, Icahn School of Medicine at Mount Sinai, New York, New York, USA

Correspondence should be addressed to K.C. (kang@wayne.edu).

[13]Present address: Department of Biology, City University of New York Kingsborough Community College, Brooklyn, New York, USA.

[14]These authors contributed equally to this work.

Note: Any Supplementary Information and Source Data files are available in the online version of the paper.

AUTHOR CONTRIBUTIONS

B.H. designed and performed the research, discussed and analyzed the data, and wrote the paper. A.N.F. designed and performed the research and analyzed the data. M.D.P., B.P., J.W.G., J.Z.Z., N.G.E.-H., J. Deng, J.L., F.Y., R.S.D., J.S.J., M.L.S., J. Dai, M.C., C.S. and L.A.P. performed the research and analyzed the data.

R.A.N., T.B.J., M.H.B. and K.S.P. provided specimens. B.G., N.R.N., E.P. and W.-Z.W. revised the manuscript. A.C. and M.C. discussed the data. K.C. conceived the study, supervised and performed the research, discussed and analyzed the data, and wrote the paper.

COMPETING FINANCIAL INTERESTS

The authors declare no competing financial interests.

Data availability. All data generated or analyzed during this study are included in this published article and its supplementary information files.

[11]Mucosal Immunology Studies Team, National Institute of Allergy and Infectious Diseases, National Institutes of Health, Bethesda, Maryland, USA

[12]Department of Pathology and Immunology, Washington University School of Medicine, St. Louis, Missouri, USA

Abstract

Preterm birth (PTB) is a leading cause of neonatal death worldwide[1]. Intrauterine and systemic infection and inflammation cause 30–40% of spontaneous preterm labor (PTL)[2], which precedes PTB. Although antibody production is a major immune defense mechanism against infection, and B cell dysfunction has been implicated in pregnancy complications associated with PTL[3,4], the functions of B cells in pregnancy are not well known[5–8]. We found that choriodecidua of women undergoing spontaneous PTL harbored functionally altered B cell populations. B cell–deficient mice were markedly more susceptible than wild-type (WT) mice to PTL after inflammation, but B cells conferred interleukin (IL)-10-independent protection against PTL. B cell deficiency in mice resulted in a lower uterine level of active progesterone-induced blocking factor 1 (PIBF1), and therapeutic administration of PIBF1 mitigated PTL and uterine inflammation in B cell–deficient mice. B cells are a significant producer of PIBF1 in human choriodecidua and mouse uterus in late gestation. PIBF1 expression by B cells is induced by the mucosal alarmin IL-33 (ref. 9). Human PTL was associated with diminished expression of the a-chain of IL-33 receptor on choriodecidual B cells and a lower level of active PIBF1 in late gestation choriodecidua. These results define a vital regulatory cascade involving IL-33, decidual B cells and PIBF1 in safeguarding term pregnancy and suggest new therapeutic approaches based on IL-33 and PIBF1 to prevent human PTL.

PTB, defined as birth before 37 weeks of gestation in humans, affects 5–18% pregnancies worldwide and has remained an intractable cause of neonatal mortality and long-term morbidity[1]. Spontaneous PTL is an immediate predecessor to PTB in most cases[1]. Intrauterine and systemic infection and inflammation are recognized pathophysiologic mechanisms that account for 30–40% of this adverse clinical condition[2]. The host immune processes in infection- or inflammation-driven PTL and PTB remain unknown. Although antibody production by B cells is an important immune defense mechanism against mucosal and systemic infection, the function of B cells in pregnancy is poorly understood. B cells have long been considered to be rare or absent from the decidua[5–8]. Maternal B cells undergo substantial modifications during pregnancy[10–13], presumably to assist the acceptance of a semi-allogeneic fetus, and B cell dysfunction has been implicated in pregnancy complications associated with PTL[3,4]. We hypothesized that B cells have a crucial role in regulating pregnancy, and sought to better define the host protective immune pathways against PTL.

By analyzing specimens of women with spontaneous term labor (TL) or PTL (Supplementary Table 1), we found that B cells were present in human choriodecidual stroma (Supplementary Fig. 1) and constituted approximately 1% and 2.5% of $CD45^+$ cells in TL and PTL cases, respectively (Fig. 1a–c). Choriodecidual B cells exhibited a distinct phenotype from that of peripheral blood B cells, with higher expression of the activated,

memory B cell–or plasma cell (PC)-associated molecules CD11c, CD27, CD38, CD70, CD80, CD86, CD95, CD138 and B cell maturation antigen (BCMA), lower expression of CD23 and C-C chemokine receptor 7 (CCR7), and a higher proportion of $CD20^{lo}$, $CD22^{lo}$, IgM^{lo} and IgD^{lo} cells (Fig. 1d **and** Supplementary Fig. 2a,b), a profile that is suggestive of higher activation, class switching, memory and plasmacytoid differentiation, and is consistent with tissue residency. Choriodecidual B cells also expressed CCR6 and the integrins α_4 and β_7, but not CCR9, and only a little CCR10 (Supplementary Fig. 2b), which promote lymphocyte homing to intestine and skin-associated mucosal tissues, respectively[14–16], indicating that B cell migration to choriodecidua involves nonoverlapping homing receptors from migration to other mucosal sites. Compared with TL choriodecidua, PTL choriodecidua harbored more B cells (Fig. 1a–c) and $CD20^{+}CD70^{-}CD43^{+}CD27^{+}$ cells (Fig. 1e–g), a population that has been postulated to be B-1 cells, which can spontaneously secrete autoreactive/polyreactive IgM[17] and has been implicated in other adverse pregnancy outcomes[3], and more $CD24^{-}CD38^{hi}$ PCs (Fig. 1h–j). The expression of several direct or indirect B cell–stimulating molecules, including B cell–activating factor of the tumor necrosis factor family (BAFF), a proliferation-inducing ligand (APRIL) and thymic stromal lymphopoietin (TSLP)[18,19], was higher in choriodecidual epithelial and/or stromal cells of PTL subjects than TL subjects (Supplementary Fig. 3a,b), which might underlie the expansion and higher activation of B cells in PTL choriodecidua. Collectively, human PTL choriodecidua harbored B cells with altered functions that were characterized by aberrant expansion, and higher activation and antibody production as compared with TL choriodecidua.

B cells produce IL-10 to suppress systemic and local inflammation[20,21], and IL-10 is crucial for protection against inflammation-induced PTL in mice[22,23]. IL-10 expression was lower in choriodecidual B cells in PTL subjects than in TL subjects (Fig. 1k,l), although the total numbers of $IL\text{-}10^{+}$ B cells were similar in TL and PTL choriodeciduas (Fig. 1m). To determine whether B cells protect against PTL triggered by inflammation, we compared the susceptibility of WT C57BL/6 mice and B cell–deficient μMT mice to PTL induced by administration of lipopolysaccharides (LPS) on gestational day (gd) 16.5, a commonly used mouse model for human PTL triggered by systemic inflammation[2]. Although WT mice were relatively resistant to PTL and had a modest level of neonatal/fetal mortality after LPS administration, μMT mice experienced markedly higher rates of PTL and neonatal/fetal mortality (Fig. 2a,b), which were accompanied by higher induction of uterine proinflammatory mediators (Fig. 2c **and** Supplementary Fig. 4a) and higher neutrophil infiltration into the uterus (Fig. 2d **and** Supplementary Fig. 4b,c). Neutrophils in the uterus of μMT mice exhibited heightened activation, including higher expression of CD11b, CD18, intercellular adhesion molecule-1 (ICAM-1), major histocompatibility complex class II (MHC-II) and inducible nitric oxide synthase (iNOS), and lower expression of CD62L (Fig. 2e **and** Supplementary Fig. 4d). The proportions of uterine $CD11b^{+}Ly\text{-}6C^{+}$ inflammatory monocytes were similar in WT and μMT mice (Supplementary Fig. 4e,f), and induction of *Ccl2* was comparable in WT and μMT uteri (Supplementary Fig. 4g). Thus, B cells protect against PTL induced by inflammation in the third trimester in mice.

To determine whether B cells confer protection against PTL by producing IL-10, we administered LPS on gd 16.5 to μMT mice that received either syngeneic WT or syngeneic *Il10*$^{-/-}$ B cells. Adoptive transfer of either WT or *Il10*$^{-/-}$ B cells restored the resistance of μMT mice to PTL (Fig. 2f), attenuated neonatal/fetal mortality (Fig. 2g) and suppressed uterine induction of pro-inflammatory mediators (Fig. 2h) and neutrophil infiltration (Fig. 2i). Consistent with IL-10-independent protection, the uterus of μMT mice showed higher *Il10* induction after LPS administration (Supplementary Fig. 5a). The induction of transforming growth factor-β (TGF-β)[24,25] and IL-35 (refs. 26,27), which contains Epstein–Barr-virus-induced gene 3 (EBI3) as a subunit[28], was similar in WT and μMT mice (Supplementary Fig. 5b). μMT mice that received WT or *Il10*$^{-/-}$ B cells also showed a similar induction of uterine *Ebi3* after LPS administration as compared to μMT mice that did not receive B cells (Supplementary Fig. 5c). Collectively, these data argue against a substantial role of IL-10, TGF-β or IL-35 in B cell–mediated protection against PTL.

Given that progesterone is important to the maintenance of term pregnancy[29], we asked whether B cells are effectors in progesterone-mediated immune regulation in late pregnancy. The progesterone-inducible molecule PIBF1 carries out many effector functions of progesterone in pregnancy[30], and a lower serum concentration of PIBF1 in late pregnancy is associated with an increased risk of human PTL[31]. Full-length 90-kDa PIBF1 is a nucleus- or centrosome-associated protein[32], whereas several alternatively spliced shorter isoforms, including the 35-, 48-, 57- and 67-kDa isoforms, can be secreted by certain tumor cells and by immune cells and trophoblasts during pregnancy, and are biologically active[32–34]. As compared with WT mice, μMT mice showed much lower active PIBF1 expression in late gestation uterus (Fig. 3a) and defective induction of uterine *Pibf1* transcript after LPS administration (Fig. 3b). However, WT and μMT mice had similar serum progesterone concentrations after LPS administration (Fig. 3c). Transfer of WT or *Il10*$^{-/-}$ B cells to μMT mice resulted in higher uterine active PIBF1 expression after LPS administration (Fig. 3d,e). These results suggest that B cells are an important source of active PIBF1 in mouse uterus in late pregnancy. Flow cytometry and immunofluorescence further revealed that mouse uterine B cells expressed PIBF1 during mid- and late gestation (Fig. 3f), and human choriodecidual B cells also expressed PIBF1 during late gestation (Fig. 3g,h and Supplementary Fig. 6a). PIBF1 in choriodecidual B cells was both concentrated perinuclearly and distributed in the cytoplasm (Fig. 3i **and** Supplementary Fig. 6b), consistent with the localization of centrosome-associated and secretory PIBF1, respectively[33]. Of note, B cells were the cell population with the highest PIBF1 expression in mouse uterus (Supplementary Fig. 7a−d) and human choriodecidua (Supplementary Fig. 8a−d). Furthermore, human peripheral blood CD19^{+} B cells contained more full-length and active PIBF1 protein than other peripheral blood mononuclear cells (PBMCs), and PBMCs depleted of B cells were almost devoid of full-length and active PIBF1 (Supplementary Fig. 8e). Thus, B cells are an important source of active PIBF1 in human choriodecidua and mouse uterus during late pregnancy.

To test whether B cell–mediated protection against PTL involves PIBF1 and whether therapeutic delivery of PIBF1 can promote resistance to PTL, we administered either phosphate-buffered saline (PBS) or recombinant human full-length PIBF1 (fPIBF1) to μMT mice before LPS challenge. As compared to PBS administration, fPIBF1 administration

significantly lowered the rates of LPS-induced preterm delivery and neonatal/fetal mortality (Fig. 3j,k), suppressed uterine induction of proinflammatory mediators (Fig. 3l **and** Supplementary Fig. 9a) and inhibited neutrophil infiltration into the uterus (Fig. 3m,n). Uterine neutrophils exhibited lower activation in fPIBF1-treated versus PBS-treated mice after LPS challenge, with lower expression of CD11b, CD18, iNOS, ICAM-1 and MHC-II, and higher expression of CD62L (Fig. 3o **and** Supplementary Fig. 9b). Administration of a recombinant C-terminal fragment of PIBF1 (cPIBF1) (Supplementary Fig. 10a) neither mitigated PTL or neonatal/fetal death (Supplementary Fig. 10b,c) nor suppressed uterine neutrophil infiltration or activation triggered by LPS (Supplementary Fig. 10d,e). Thus, supplementation of PIBF1 promotes resistance to LPS-induced PTL in μMT mice, and the protective activity of PIBF1 resides in its N terminus.

We further sought to understand the regulation of PIBF1 expression by B cells and tested a panel of cytokines known to modulate B cell function. We performed quantitative real-time PCR and western blot analyses and found that IL-33 promoted PIBF1 expression by human peripheral blood B cells, similar to progesterone[35] (Fig. 4a,b). By contrast, interferon-γ (IFN-γ), IL-17A, IL-10 and TGF-β had no effect, and tumor necrosis factor (TNF) had a suppressive effect (Supplementary Fig. 11a). Of note, among the T helper type 2 (T_H2) cytokines tested, including IL-4, IL-25, TSLP and IL-33, only IL-33 induced PIBF1 expression by human B cells (Supplementary Fig. 11a). Indeed, human peripheral blood or choriodecidual B cells did not express the receptors for IL-25 or TSLP (Supplementary Fig. 11b). PIBF1 expression by mouse uterine B cells during late pregnancy was also dependent on IL-33, as PIBF1 was diminished in the uteri and uterine B cells of *Il33*$^{-/-}$ mice in late gestation (Fig. 4c,d and Supplementary Fig. 12a–d). Consistently, mouse uterine PIBF1 level did not decrease during progesterone withdrawal in late pregnancy (Supplementary Fig. 13a,b). Thus, PIBF1 expression in mouse late gestation was maintained largely by IL-33 rather than progesterone.

IL-33 is a mucosal alarmin that signals tissue damage following stress or infection[9], and that can induce immune cells with regulatory functions to maintain tissue homeostasis[36–40]. Given that uterine stress and infection are causally linked to human PTL[2], we asked whether human PTL encompasses defects in this protective pathway involving IL-33, decidual B cells and PIBF1. Although human peripheral blood and choriodecidual B cells constitutively expressed the β-chain of IL-33 receptor (IL-33R), interleukin-1 receptor accessory protein (IL1RAcP; Supplementary Fig. 14a–c), the expression of the IL-33R α-chain, interleukin-1 receptor-like 1 (ST2L), was significantly lower on choriodecidual B cells in PTL subjects than in TL subjects (Fig. 4e–i). PIBF1 expression in choriodecidua and choriodecidual B cells of subjects with PTL was concomitantly diminished (Fig. 4h–j). The lower expression of PIBF1 or ST2L on choriodecidual B cells was unlikely to be a result of a lower choriodecidual progesterone level, because TL and PTL choriodecidual tissues contained similar levels of progesterone at delivery (Supplementary Fig. 15a). Consistently, progesterone treatment did not lead to higher ST2L expression on cultured human B cells (Supplementary Fig. 15b). Thus, human PTL is associated with defects in IL-33 responsiveness of and PIBF1 production by choriodecidual B cells independently of progesterone.

Taken together, our findings reveal an axis of B cell–mediated immune regulation that involves IL-33-dependent expression of PIBF1 and uncover a long-neglected, but vital, role of B cells in safeguarding term pregnancy that is defective in PTL (Fig. 4k). Of note, although PIBF1 is recognized as a progesterone-induced molecule, our findings indicate that B cell–derived PIBF1 goes beyond being a progesterone effector molecule and has an important role in promoting tissue homeostasis in response to tissue stress independently of progesterone. The identification of this B cell–mediated protective pathway suggests new therapeutic strategies involving IL-33 and PIBF1 for the prevention and treatment of human PTL.

ONLINE METHODS

Study subjects

Women who underwent spontaneous TL (37–41 weeks of gestation) or spontaneous PTL (between 32–37 weeks of gestation) (Supplementary Table 1) were enrolled in this study with written informed consent at Oakwood Hospital of Beaumont Healthcare System and the affiliated hospitals of the Detroit Medical Center (DMC) under protocols approved by the Institutional Review Board of Wayne State University, Oakwood Hospital and the DMC. Subjects with a current diagnosis of pre-eclampsia, a prior history or current diagnosis of diabetes, chronic hypertension, asthma, thyroid disease, pyelonephritis, active chlamydia, gonorrhea or syphilis infections, active HPV or HSV lesions, HIV infection and/or recreational drug use were excluded.

Human blood and tissue samples

Placentas and the attached chorioamniotic membranes were obtained after delivery. In each case, several random strips of the chorioamniotic membranes located at different regions of the choriodecidua were embedded in rolls in optimal cutting temperature (OCT) compound (Sakura Finetek 4583), frozen in liquid nitrogen and stored at −80 °C for immunofluorescence analysis. Choriodecidual tissues were scraped from the chorionic membranes that had blood clots removed, and digested with 0.2% (w/v) *Clostridium histolyticum* collagenase V (Sigma-Aldrich C9263) in RPMI-1640 with 10% FBS (Thermo Fisher Scientific 26140-079) at 37 °C with gentle agitation for 45 min. Cells released from the tissues were cleaned by being passed through a 100-μm cell strainer and centrifuged on a Ficoll gradient. Peripheral blood leukocytes of anonymous healthy donors after leukophoresis were obtained from the Southeast Michigan branch of American Red Cross with a protocol approved by the Institutional Review Board of Wayne State University and the DMC. Peripheral blood mononuclear cells (PBMCs) were isolated using Histopaque-1077 (Sigma-Aldrich 10771) following the manufacturer's instructions. Red blood cells were lysed using an ammonium-chloride-potassium lysing buffer (Thermo Fisher Scientific A1049201). IgD^+ B cells were purified from PBMCs by magnetic-activated cell sorting with a biotinylated goat $F(ab')_2$ anti-human IgD antibody and anti-biotin magnetic microbeads (Miltenyi Biotec), as previously reported[41]. The purity of the IgD^+ B cells ranged from 92–99% as determined by flow cytometry with CD19 staining. $CD19^+$ B cells were similarly separated from PBMCs using a biotinylated mouse anti-human CD19 (clone

HIB19) antibody, with purity ranging from 93–97% as determined by flow cytometry using a different clone (SJ25C1) of CD19 antibody.

Mice

C57BL/6 mice (Jackson stock number 000664), Balb/c mice (Jackson stock number 000651), μMT (B6.129S2-*Ighm*^{tm1Cgn}, Jackson stock number 002288) and *Il10*$^{-/-}$ (B6.129P2-Il10^{tm1Cgn}, Jackson stock number 002251) mice in C57BL/6 background were purchased from the Jackson Laboratory. *Il33*$^{-/-}$ *lacZ* reporter mice in the C57BL/6 background were generated by the mouse core of the NIH/NIAID Mucosal Immunology Studies Team at Washington University School of Medicine. All mice were maintained in the same specific-pathogen-free facility of the Division of Laboratory Animal Resources of Wayne State University. All protocols were approved by Wayne State University Institutional Animal Care and Use Committee.

Mouse models of preterm labor

6–10-week-old virgin female C57BL/6 (WT) or μMT mice were mated with male Balb/c mice. Female mice were examined daily in the early morning for the presence of a vaginal plug, which denoted gd 0.5. In the late morning of gd 16.5, pregnant female mice were intraperitoneally administered with 200 μl of sterile PBS or 200 μl of sterile PBS containing 0.5, 2.5, 5, 10 or 20 μg LPS from *Salmonella enterica* serotype typhimurium (Sigma-Aldrich L6143). The various doses of LPS were assigned to the mice randomly. In some experiments, splenic B cells of 5–8-week-old virgin female WT or *Il10*$^{-/-}$ mice were purified using a mouse resting B cell negative isolation kit (Miltenyi Biotec 130-090-862) to 94–99% purity as determined by CD19 staining. 10^7 purified B cells were adoptively transferred in 200 μl sterile PBS into pregnant female μMT mice on gd 14.5 before LPS administration on gd 16.5. In some other experiments, 200 μl sterile PBS or 200 μl sterile PBS containing 1 μg recombinant full-length PIBF1 (fPIBF1) (aa 1–755, with an N-terminal glutathione-S-transferase (GST) tag, Abnova H00010464-P01) or 300 ng of a recombinant C-terminal fragment of PIBF1 (cPIBF1) (aa 660–755, with an N-terminal glutathione-*S*-transferase (GST) tag, Abnova H00010464-Q01) was intravenously administered to pregnant female μMT mice on gd 16.5 3 h before intraperitoneal LPS administration. 24 h after LPS administration, female mice were examined for delivery and death of delivered pups if delivery occurred. They were then killed for the examination of neonatal/fetal mortality, which was calculated as the total number of dead delivered pups and dead fetuses divided by the total number of implantation sites. Uteri were collected, briefly washed in PBS and processed for RNA and protein extraction or flow cytometry. The people performing the analysis were not blinded to the genotype or treatment of the mice.

Cell culture

Human PMBCs, IgD$^+$ B cells, CD19$^+$ B cells or PBMCs depleted of CD19$^+$ B cells were cultured in RPMI-1640 medium (Sigma-Aldrich R8578) supplemented with 2 mM L-glutamine, 2 mg/ml $NaHCO_3$, 100 U/ml penicillin, 100 μg/ml streptomycin, 0.25 μg/ml amphotericin B and 10% FBS. Cells were stimulated with 1 μM progesterone (Sigma-Aldrich P0130), or 100 ng/ml IL-33 (R&D 3625-IL-010 or Peprotech 200-33), IL-4 (Peprotech 200-04), IL-10 (Peprotech 200-10), IL-17A (Peprotech 200-17), IL-25 (R&D

1258-IL-025), IFN-γ (Peprotech 300-02), TSLP (Peprotech 300-62), or 1 ng/ml TGF-β (R&D 240-B-010/CF), or 50 ng/ml TNF (210-TA-020). RNA or protein expression was analyzed after 3 d. The primary cell cultures were not tested for mycoplasma infection.

RNA extraction and quantitative real-time polymerase chain reaction

RNA was extracted from cells or tissues using TRIzol (Thermo Fisher Scientific 15596026). cDNA synthesis was performed using the Superscript III first-strand synthesis system (Thermo Fisher Scientific 188080051) in a thermocycler (Bio-Rad T100). Quantitative real-time PCR was performed with Power SYBR Green PCR Master Mix (Thermo Fisher Scientific 4367660) in a StepOnePlus instrument (Applied Biosystems) using pairs of sense and anti-sense primers targeted at the genes of interest (Supplementary Table 2).

Flow cytometry and cell sorting

Cells were incubated with an Fc blocking reagent and stained at 4 °C with antibodies to various cell surface antigens (Supplementary Table 3). For staining of intracellular molecules, cells were subsequently fixed and permeabilized using a CytoFix/CytoPerm kit (BD 554722). Isotype-matched control antibodies were used to define the baseline staining for the molecules of interest. Cells or beads stained with each fluorochrome were used to establish fluorescent compensation. 7-aminoactinomycin D (7-AAD, Tonbo Biosciences 13-6993-T500 or BD Biosciences 559925) or Ghost Dye Violet 510 (Tonbo Biosciences 13-0870-T500) was used to identify dead cells in order to exclude them from the analysis. Events were acquired on an LSR II, LSRFortessa or FACSCanto II cytometer (BD Biosciences) and analyzed by FlowJo (Tree Star). In some experiments, stained cells were sorted using a SONY SH800 or SY3200 cell sorter (SONY Biotechnology).

Imaging flow cytometry

Choriodecidual cell suspensions were incubated with an Fc blocking reagent and stained at 4 °C with antibodies to various surface antigens, fixed and permeabilized, and stained for PIBF1 or with an isotype control antibody, followed by a fluorochrome-conjugated secondary antibody (Supplementary Table 3). Nuclei were counter stained with Hoechst 33342 (Thermo Fisher Scientific 62249). Cells or beads stained with each fluorochrome were used to establish fluorescent compensation. Cells were imaged on an ImageStream X Mark II imaging flow cytometer (Amnis) and data were analyzed using IDEAS 6.1 (Amnis).

Immunohistochemistry

Frozen human tissues were stored at −80 °C shortly before sectioning. 6–7-μm tissue sections were made using a cryostat (Leica CM1950). Sections were fixed with 4% paraformaldehyde, permeabilized in PBS containing 0.2% Triton X-100, blocked with PBS containing 10 mg/ml bovine serum albumin (BSA) and 100 μg/ml human IgG. Endogenous biotin was subsequently blocked with an Avidin/Biotin blocking kit (Thermo Fisher Scientific 004303). The tissues were stained with primary antibodies against target antigens isotype control antibodies from the same company with the same conjugation, if the primary antibody is conjugated followed by alkaline-phosphatase- or horseradish-peroxidase-conjugated secondary antibodies (Supplementary Table 3). Single-color reactions were

developed by using 3,3′-diaminobenzidine as the substrate (Vector Laboratories SK-4105), whereas dual-color reactions were developed using 5-bromo-4-chloro-3-indolyl phosphate/nitro blue tetrazolium (Sigma-Aldrich B5655) and 3-amino-9-ethylcarbazole (Sigma-Aldrich AEC101) as substrates. Nuclei were visualized with hematoxylin on single-color slides. Slides were imaged using an Olympus BX40 or Nikon TE-2000 microscope with CellSens Dimension software.

Immunofluorescence

Frozen human tissues were stored at −80 °C shortly before sectioning. 6–7-μm tissue sections were made using a cryostat (Leica CM1950). Sections were fixed with 4% paraformaldehyde, permeabilized in PBS containing 0.2% Triton X-100, blocked with PBS containing 10 mg/ml bovine serum albumin (BSA), 100 μg/ml human IgG and 10% serum from the source of the fluorochrome-conjugated antibodies, and stained with various combinations of primary antibodies against the molecules of interest, followed by appropriate fluorochrome-conjugated secondary antibodies (Supplementary Table 3). Nuclei were visualized with 4′,6-diamidine-2′-phenylindole dihydrochloride (DAPI, Sigma-Aldrich D9542). Following washing, slides were mounted using a FluoroSave reagent (EMD Millipore 345789) and imaged using a confocal microscope. Pseudocolor images were processed using Photoshop (Adobe).

Protein extraction and western blot

Cells were pelleted and washed twice with cold PBS and lysed in a pH 8.0 protein extraction buffer containing 20 mM Tris-HCl, 150 mM NaCl, 1% IGEPAL CA-630 (Sigma-Aldrich I8896), 0.1% sodium dodecyl sulfate (SDS), 1 mM EDTA and protease and phosphatase inhibitor cocktail on ice for 30 min. For protein extraction from mouse uterus and human chorioamniotic membranes, the tissue was washed twice with PBS to remove blood and homogenized in the above protein-extraction buffer with a tissue tearor (Biospec Products 985370), followed by three rounds of sonication at 30% maximum power for 5 s per round using a sonifier (Thermo Fisher Scientific Q500). Supernatants were collected after centrifugation, heated at 98 °C in an SDS buffer with 4% β-mecaptoethanol for 5 min to denature proteins. Proteins were resolved in 4–20% Bis-Tris gels (GenScript M42012) and transferred to 0.45 μm nitrocellulose membranes (Bio-Rad 1620115). The membranes were blocked with 5% (w/v) non-fat milk in Tris-buffered saline with Tween-20 for 30 min, incubated with primary antibodies overnight at 4 °C and subsequently with secondary antibodies conjugated to horseradish peroxidase (Supplementary Table 3). Signals were visualized with clarity western-blot ECL substrate (Bio-Rad 170-5061) and exposed on autoradiograph films. Cropped blot images were shown in the figures, with full-length blots shown in the supplementary information.

Enzyme-linked immunosorbent assay (ELISA)

Progesterone levels in sera and tissues were determined using an ELISA kit (Cayman Chemical 582601) according to the manufacturer’s instruction.

Statistical analysis

The sample size was calculated on the basis of the effect size derived from preliminary data at 5% significance level and 80% power using the software G*Power 3.1. Sample availability exceeded the estimated sample size. Results are expressed as mean ± s.e.m. Percentage data were subjected to square-root transformation before statistical analysis to verify test assumptions of equal variance. Statistical difference in the rate of PTL between different strains of mice or different treatment groups was assessed by Fisher's exact test. Statistical difference in neonatal/fetal mortality was assessed by Mann–Whitney U test. For flow cytometry and RT–qPCR data, Shapiro–Wilk test was used to determine the normality of the data. Statistical significance was assessed by Student's t test for normally distributed data and Mann–Whitney U test for non-normally distributed data. $P < 0.05$ was considered to be statistically significant.

Supplementary Material

Refer to Web version on PubMed Central for supplementary material.

Acknowledgments

We thank the European Conditional Mouse Mutagenesis Program and Barry Rosen (Wellcome Trust Sanger Institute) for mouse *Il33* targeting vectors, the NIAID Mucosal Immunology Studies Team (MIST) mouse core for generating the *Il33*$^{-/-}$ *lacZ* reporter mice, and M. Treadwell (University of Michigan at Ann Arbor) and W. Xu (Bristol-Myers Squibb) for discussion of the manuscript. This study was supported by grants from the Burroughs Wellcome Fund (Preterm Birth Initiative), US National Institutes of Health (U01AI95776 MIST Young Investigator Award, R21AI122256, P30CA22453), American Congress of Obstetricians and Gynecologists and Wayne State University (Perinatal Initiative) (to K.C.). A.N.F. was partially supported by a fellowship from the Wayne State University Office of the Vice President for Research.

References

1. Goldenberg RL, Culhane JF, Iams JD, Romero R. Epidemiology and causes of preterm birth. Lancet. 2008; 371:75–84. [PubMed: 18177778]
2. Romero R, et al. The preterm parturition syndrome. BJOG. 2006; 113(Suppl. 3):17–42.
3. Jensen F, et al. CD19^{+}CD5^{+} cells as indicators of preeclampsia. Hypertension. 2012; 59:861–868. [PubMed: 22353610]
4. Zhou CC, et al. Angiotensin receptor agonistic autoantibodies induce pre-eclampsia in pregnant mice. Nat. Med. 2008; 14:855–862. [PubMed: 18660815]
5. Matthiesen, L., et al. Immunology of preeclampsia. In: Markert, UR., editor. Immunology of Pregnancy. Vol. 89. Karger, Basel: 2005. p. 49-61.
6. Frank, HG., Kaufmann, P. Nonvillous parts and trophoblast invasion. In: Benirschke, K.Kaufmann, P., Baergen, RN., editors. Pathology of the Human Placenta. Springer; New York, NY: 2006. p. 191-287.
7. Trundley A, Moffett A. Human uterine leukocytes and pregnancy. Tissue Antigens. 2004; 63:1–12. [PubMed: 14651517]
8. Moffett A, Shreeve N. First do no harm: uterine natural killer (NK) cells in assisted reproduction. Hum. Reprod. 2015; 30:1519–1525. [PubMed: 25954039]
9. Martin NT, Martin MU. Interleukin 33 is a guardian of barriers and a local alarmin. Nat. Immunol. 2016; 17:122–131. [PubMed: 26784265]
10. Muzzio DO, et al. B cell development undergoes profound modifications and adaptations during pregnancy in mice. Biol. Reprod. 2014; 91:115. [PubMed: 25210132]

11. Zimmer JP, Garza C, Butte NF, Goldman AS. Maternal blood B-cell ($CD19^+$) percentages and serum immunoglobulin concentrations correlate with breast-feeding behavior and serum prolactin concentration. Am. J. Reprod. Immunol. 1998; 40:57–62. [PubMed: 9689362]
12. Bhat NM, Mithal A, Bieber MM, Herzenberg LA, Teng NN. Human $CD5^+$ B lymphocytes (B-1 cells) decrease in peripheral blood during pregnancy. J. Reprod. Immunol. 1995; 28:53–60. [PubMed: 7537825]
13. Medina KL, Kincade PW. Pregnancy-related steroids are potential negative regulators of B lymphopoiesis. Proc. Natl. Acad. Sci. USA. 1994; 91:5382–5386. [PubMed: 8202495]
14. Reiss Y, Proudfoot AE, Power CA, Campbell JJ, Butcher EC. CC chemokine receptor (CCR)4 and the CCR10 ligand cutaneous T cell-attracting chemokine (CTACK) in lymphocyte trafficking to inflamed skin. J. Exp. Med. 2001; 194:1541–1547. [PubMed: 11714760]
15. Mora JR, et al. Selective imprinting of gut-homing T cells by Peyer's patch dendritic cells. Nature. 2003; 424:88–93. [PubMed: 12840763]
16. Homey B, et al. CCL27-CCR10 interactions regulate T cell-mediated skin inflammation. Nat. Med. 2002; 8:157–165. [PubMed: 11821900]
17. Griffin DO, Holodick NE, Rothstein TL. Human B1 cells in umbilical cord and adult peripheral blood express the novel phenotype $CD20^+$ $CD27^+$ $CD43^+$ $CD70^-$. J. Exp. Med. 2011; 208:67–80. [PubMed: 21220451]
18. Litinskiy MB, et al. DCs induce CD40-independent immunoglobulin class switching through BLyS and APRIL. Nat. Immunol. 2002; 3:822–829. [PubMed: 12154359]
19. Xu W, et al. Epithelial cells trigger frontline immunoglobulin class switching through a pathway regulated by the inhibitor SLPI. Nat. Immunol. 2007; 8:294–303. [PubMed: 17259987]
20. Candando KM, Lykken JM, Tedder TF. B10 cell regulation of health and disease. Immunol. Rev. 2014; 259:259–272. [PubMed: 24712471]
21. Rosser EC, Mauri C. Regulatory B cells: origin, phenotype, and function. Immunity. 2015; 42:607–612. [PubMed: 25902480]
22. Robertson SA, Skinner RJ, Care AS. Essential role for IL-10 in resistance to lipopolysaccharide-induced preterm labor in mice. J. Immunol. 2006; 177:4888–4896. [PubMed: 16982931]
23. Thaxton JE, Romero R, Sharma S. TLR9 activation coupled to IL-10 deficiency induces adverse pregnancy outcomes. J. Immunol. 2009; 183:1144–1154. [PubMed: 19561095]
24. Tian J, et al. Lipopolysaccharide-activated B cells down-regulate Th1 immunity and prevent autoimmune diabetes in nonobese diabetic mice. J. Immunol. 2001; 167:1081–1089. [PubMed: 11441119]
25. Parekh VV, et al. B cells activated by lipopolysaccharide, but not by anti-Ig and anti-CD40 antibody, induce anergy in $CD8^+$ T cells: role of TGF-beta 1. J. Immunol. 2003; 170:5897–5911. [PubMed: 12794116]
26. Shen P, et al. IL-35-producing B cells are critical regulators of immunity during autoimmune and infectious diseases. Nature. 2014; 507:366–370. [PubMed: 24572363]
27. Wang RX, et al. Interleukin-35 induces regulatory B cells that suppress autoimmune disease. Nat. Med. 2014; 20:633–641. [PubMed: 24743305]
28. Collison LW, et al. The inhibitory cytokine IL-35 contributes to regulatory T-cell function. Nature. 2007; 450:566–569. [PubMed: 18033300]
29. Romero R, Yeo L, Chaemsaithong P, Chaiworapongsa T, Hassan SS. Progesterone to prevent spontaneous preterm birth. Semin. Fetal Neonatal Med. 2014; 19:15–26. [PubMed: 24315687]
30. Szekeres-Bartho J, Polgar B. PIBF: the double edged sword. Pregnancy and tumor. Am. J. Reprod. Immunol. 2010; 64:77–86. [PubMed: 20367622]
31. Hudić I, et al. Maternal serum progesterone-induced blocking factor (PIBF) in the prediction of preterm birth. J. Reprod. Immunol. 2015; 109:36–40. [PubMed: 25818991]
32. Polgar B, et al. Molecular cloning and immunologic characterization of a novel cDNA coding for progesterone-induced blocking factor. J. Immunol. 2003; 171:5956–5963. [PubMed: 14634107]
33. Lachmann M, et al. PIBF (progesterone induced blocking factor) is overexpressed in highly proliferating cells and associated with the centrosome. Int. J. Cancer. 2004; 112:51–60. [PubMed: 15305375]

34. Gonzalez-Arenas A, Valadez-Cosmes P, Jimenez-Arellano C, Lopez-Sanchez M, Camacho-Arroyo I. Progesterone-induced blocking factor is hormonally regulated in human astrocytoma cells, and increases their growth through the IL-4R/JAK1/STAT6 pathway. J. Steroid Biochem. Mol. Biol. 2014; 144(Pt B):463–470. [PubMed: 25218441]

35. Szekeres-Bartho J, et al. The mechanism of the inhibitory effect of progesterone on lymphocyte cytotoxicity. I. Progesterone-treated lymphocytes release a substance inhibiting cytotoxicity and prostaglandin synthesis. Am. J. Reprod. Immunol. Microbiol. 1985; 9:15–18. [PubMed: 3863495]

36. Schiering C, et al. The alarmin IL-33 promotes regulatory T-cell function in the intestine. Nature. 2014; 513:564–568. [PubMed: 25043027]

37. Sattler S, et al. IL-10-producing regulatory B cells induced by IL-33 (Breg(IL-33)) effectively attenuate mucosal inflammatory responses in the gut. J. Autoimmun. 2014; 50:107–122. [PubMed: 24491821]

38. Burzyn D, et al. A special population of regulatory T cells potentiates muscle repair. Cell. 2013; 155:1282–1295. [PubMed: 24315098]

39. Bapat SP, et al. Depletion of fat-resident T_{reg} cells prevents age-associated insulin resistance. Nature. 2015; 528:137–141. [PubMed: 26580014]

40. Arpaia N, et al. A distinct function of regulatory T cells in tissue protection. Cell. 2015; 162:1078–1089. [PubMed: 26317471]

41. Chen K, et al. Immunoglobulin D enhances immune surveillance by activating antimicrobial, proinflammatory and B cell-stimulating programs in basophils. Nat. Immunol. 2009; 10:889–898. [PubMed: 19561614]

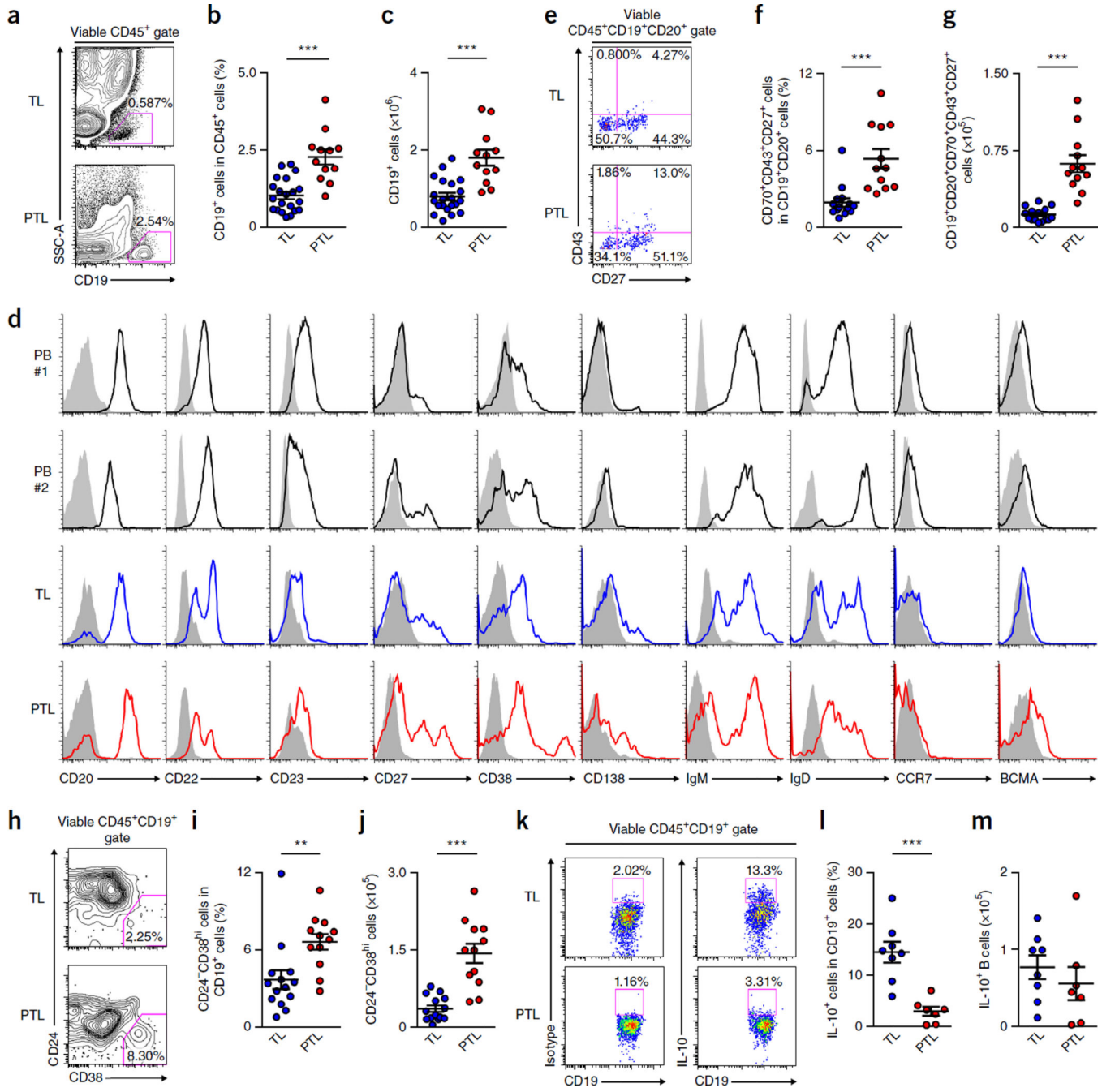

Figure 1.

Human choriodecidua harbors B cells that are dysregulated in PTL. (**a,b**) Frequency of $CD19^+$ B cells in $CD45^+$ cells in choriodecidua of women with TL ($n = 21$) or PTL ($n = 12$). (**c**) Calculated numbers of $CD19^+$ B cells recovered from choriodecidual tissues of women with TL ($n = 21$) or PTL ($n = 12$). (**d**) Expression of CD20, CD22, CD23, CD27, CD38, CD138, IgM, IgD, CCR7 and BCMA on $CD19^+$ B cells in peripheral blood (PB) of two nonpregnant healthy donors (black histogram) and choriodecidual tissues of women with TL (blue histogram) or PTL (red histogram). Shaded histograms indicate the staining of $CD19^+$

B cells in the respective tissues using isotype control antibodies. The results summarize the profiles of 20 healthy blood donors, 16 women with TL and 12 women with PTL. (**e,f**) CD43 and CD27 expression on $CD19^+CD20^+CD70^-$ B cells and the percentage of $CD19^+CD20^+CD70^-CD43^+CD27^+$ cells in $CD19^+CD20^+$ B cells in choriodecidual tissues of women with TL ($n = 15$) or PTL ($n = 12$). (**g**) Calculated total numbers of $CD19^+CD20^+CD70^-CD43^+CD27^+$ cells recovered from choriodecidual tissues of women with TL ($n = 15$) or PTL ($n = 12$). (**h,i**) CD24 and CD38 expression on $CD19^+$ B cells and the frequency of $CD24^-CD38^{hi}$ PCs in $CD19^+$ B cells in choriodecidual tissues of women with TL ($n = 14$) or PTL ($n = 12$). (**j**) Calculated total numbers of $CD24^-CD38^{hi}$ PCs recovered from choriodecidual tissues of women with TL ($n = 14$) or PTL ($n = 12$). (**k,l**) Frequency of IL-10^+ B cells in $CD19^+$ B cells in choriodecidual tissues of women with spontaneous TL ($n = 8$) or spontaneous PTL ($n = 7$). (**m**) Calculated total numbers of IL-10^+ B cells recovered from choriodecidual tissues of women with TL ($n = 8$) or PTL ($n = 7$). $^{**}P < 0.01$, $^{***}P < 0.001$, by two-tailed *t* test (**b,c,g,i,j,l,m**) or two-tailed Mann–Whitney *U* test (**f,i**).

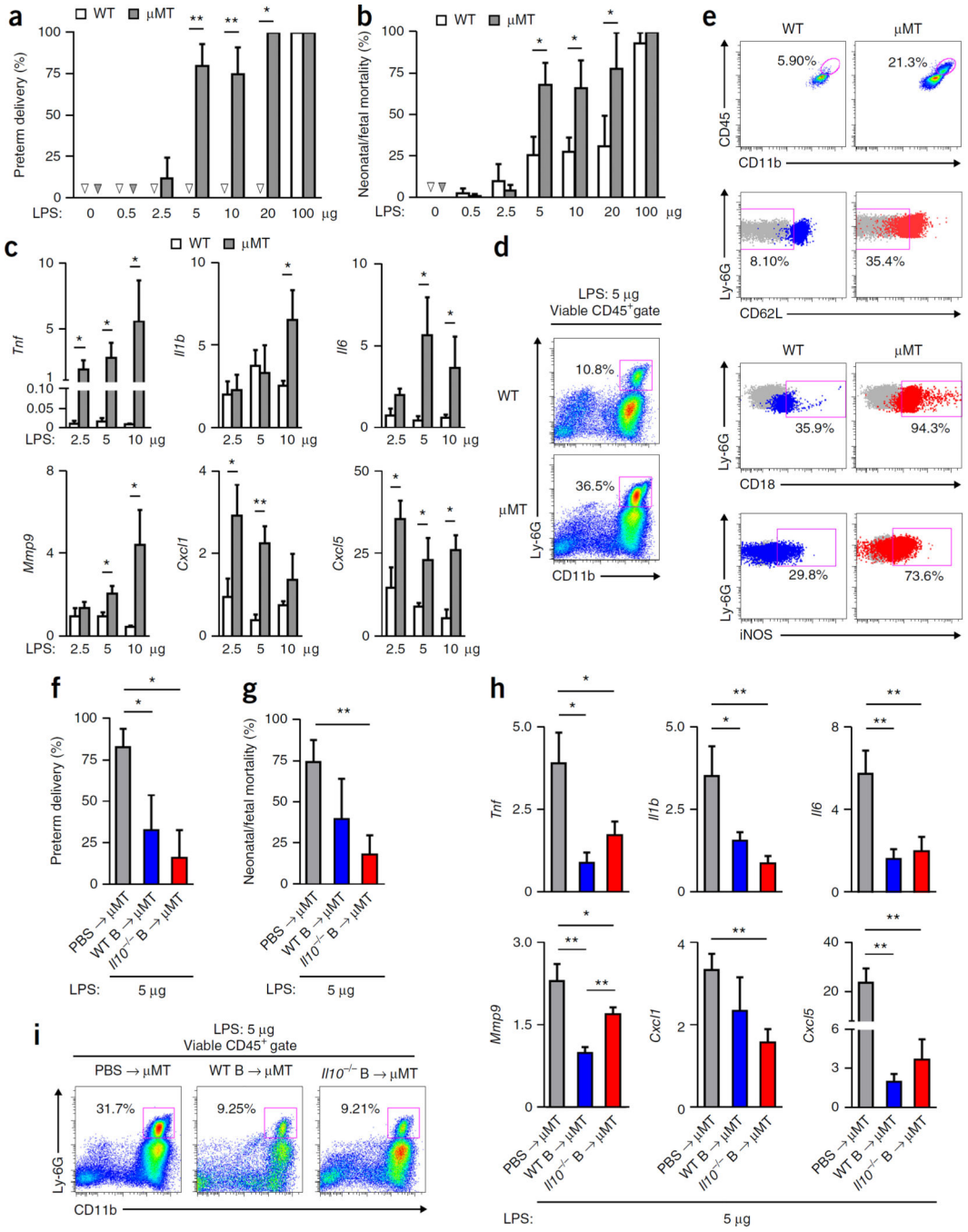

Figure 2.

B cells confer resistance to inflammation-associated PTL independently of IL-10. (**a,b**) Rates of preterm delivery and neonatal/fetal mortality of WT or μMT mice 24 h after receiving LPS administered on gd 16.5. Arrowheads indicate no PTL or neonatal/fetal mortality. (**c**) Fold change of *Tnf, Il1b, Il6, Mmp9, Cxcl1* and *Cxcl5* transcripts in uterine tissues of WT or μMT mice 24 h after receiving LPS, relative to the gene transcripts in uterine tissues of the respective strain of mice that did not receive LPS. (**d**) Frequency of $CD11b^{+}Ly\text{-}6G^{+}$ neutrophils in $CD45^{+}$ cells in uterine tissues of representative WT and μMT

mice 24 h after receiving 5 μg LPS. (**e**) Expression of surface CD11b, CD18, CD62L and intracellular iNOS by viable neutrophils in uterine tissues of a WT or μMT mouse 24 h after receiving 5 μg LPS. (**f,g**) Rate of preterm delivery and neonatal/fetal mortality on gd 17.5 of μMT mice that received either PBS or WT or *Il10*$^{-/-}$ B cells on gd 14.5 and 5 μg LPS on gd 16.5. (**h**) Fold change of *Tnf, Il1b, Il6, Mmp9, Cxcl1* and *Cxcl5* transcripts in uterine tissues of gd 17.5 μMT mice after receiving either PBS or WT or *Il10*$^{-/-}$ B cells on gd 14.5 and 5 μg LPS, relative to the gene transcripts in uterine tissues of the respective mice that did not receive LPS. (**i**) Frequency of CD11b^{+}Ly-6G^{+} neutrophils in CD45^{+} cells in uterine tissues of gd 17.5 μMT mice after receiving either PBS or WT or *Il10*$^{-/-}$ B cells on gd 14.5 and 5 μg LPS on gd 16.5. (**j**) Fold change of *Il10, Tgfb1* and *Ebi3* transcripts in uterine tissues of WT or μMT mice 24 h after receiving the indicated dose of LPS, relative to the gene transcripts in uterine tissues of the respective mice that did not receive LPS. Data in **a** and **b** represent the results of six WT mice (PBS, 0.5 and 10 μg LPS groups), seven WT mice (2.5 and 5 μg LPS groups), four WT mice (20 μg LPS group), five μMT mice (PBS and 20 μg LPS groups), eight μMT mice (2.5 and 10 μg LPS groups), nine μMT mice (0.5 μg LPS group), ten μMT mice (5 μg LPS group) or four WT or μMT mice (100 μg LPS group) per group. Data in **c** represent the results of five mice per group. Data in **d** and **e** represent the results of seven WT mice and nine μMT mice. Data in **f–i** represent the results of five mice per group. *$P < 0.05$, **$P < 0.01$, by Fisher's exact test (**a,f**), one-tailed Mann–Whitney *U* test (**b,g**) or one-tailed *t* test (**c,h**).

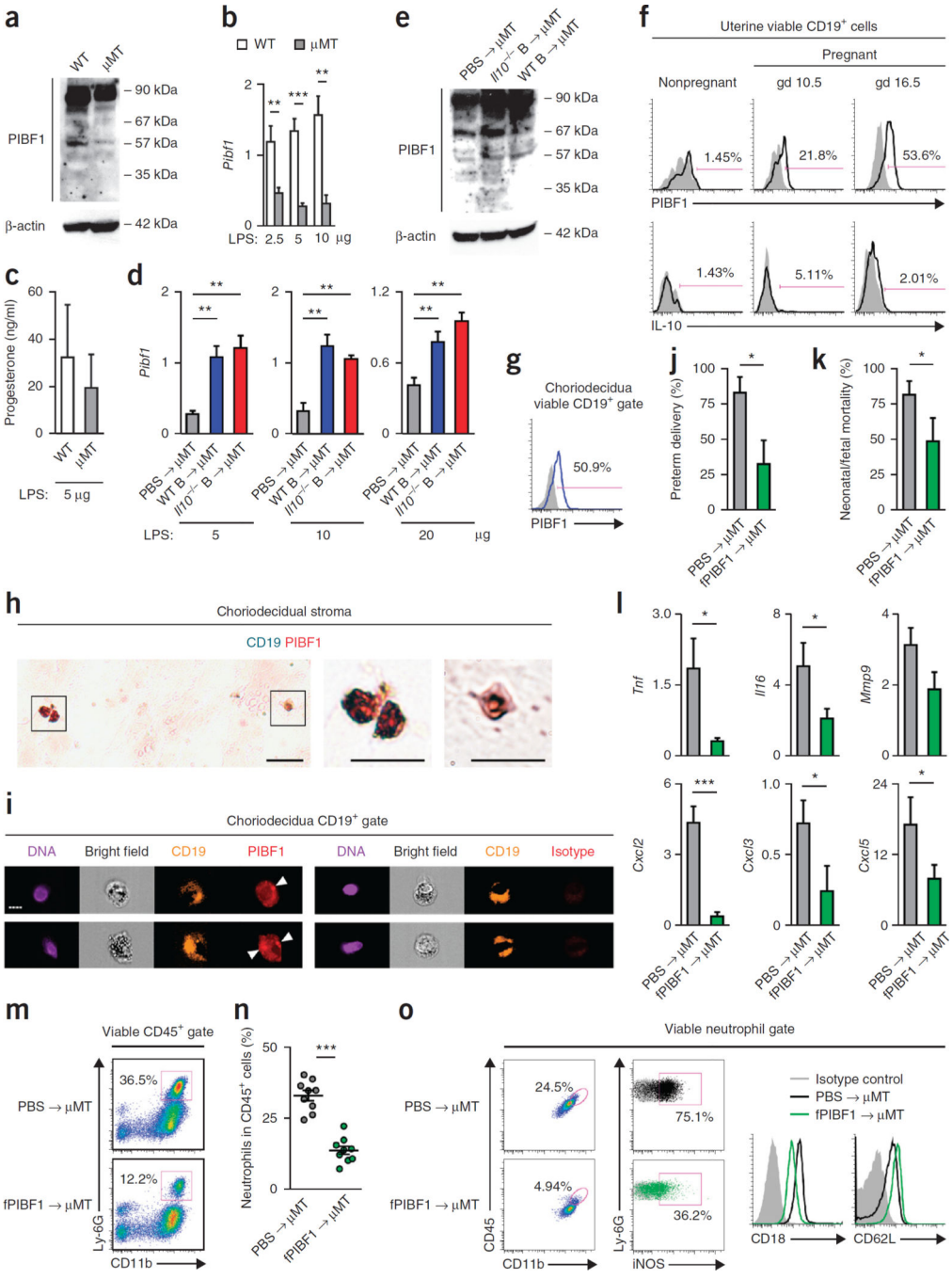

Figure 3.

B cells protect against PTL via PIBF1-dependent suppression of uterine inflammation. (**a**) Western blot analysis ($n = 3$) of PIBF1 in uterine tissues of WT or µMT mice on gd 16.5. (**b**) Fold change of *Pibf1* transcript in uterine tissues of WT or µMT mice 24 h after receiving LPS given on gd 16.5, relative to the gene transcripts in uterine tissues of the respective mice that did not receive LPS. (**c**) ELISA of serum progesterone concentrations in WT and µMT mice 24 h after 5 µg LPS challenge. (**d**) Fold change of *Pibf1* transcript in uterine tissues of gd 17.5 µMT mice after receiving either PBS or WT or *Il10*$^{-/-}$ B cells on gd 14.5 and 5 µg

LPS on gd 16.5, relative to the gene transcripts in uterine tissues of the respective mice that did not receive LPS. (**e**) Western blot analysis ($n = 3$) of PIBF1 in uterine tissues of μMT mice on gd 16.5 that received WT or *Il10*$^{-/-}$ B cells on gd 14.5. (**f**) Flow cytometry analysis of Pibf1 and IL-10 expression by uterine CD19^{+} B cells in nonpregnant WT mice and pregnant WT mice on gd 10.5 or 16.5. (**g**) Flow cytometric analysis of PIBF1 expression by choriodecidual CD19^{+} B cells in a woman with TL. (**h**) Immunohistochemical analysis of TL choriodecidual stroma for CD19 (turquoise) and PIBF1 (red). Scale bars, 20 μm. (**i**) Imaging flow cytometry analysis of PIBF1 expression by TL choriodecidual CD19^{+} B cells. Arrowheads point to concentrated perinuclear PIBF1 staining. Scale bar, 7 μm. (**j,k**) Rates of preterm delivery and neonatal/fetal mortality on gd 17.5 of μMT mice that received either PBS or fPIBF1 and 5 μg LPS on gd 16.5. (**l**) Fold change of *Tnf, Il6, Mmp9, Cxcl2, Cxcl3* and *Cxcl5* transcripts in uterine tissues of μMT mice 24 h after PBS or fPIBF1 administration and 5 μg LPS, relative to the gene transcripts in uterine tissues of the mice that received PIBF1 but not LPS. (**m,n**) Frequency of CD11b^{+}Ly-6G^{+} neutrophils in CD45^{+} cells in uterine tissues of gd 17.5 μMT mice after receiving either PBS or fPIBF1 and LPS on gd 16.5. (**o**) Expression of surface CD11b, CD18, CD62L and intracellular iNOS by viable neutrophils in uterine tissues of a μMT mouse 24 h after receiving PBS or fPIBF1 and LPS. Data represent the results from five (**a–f**) or nine mice (**j–o**) per group. $*P < 0.05$, $**P < 0.01$, $***P < 0.001$, by Fisher's exact test (**j**), one-tailed Mann–Whitney *U* test (**k**) or one-tailed *t* test (**b,d,l,n**).

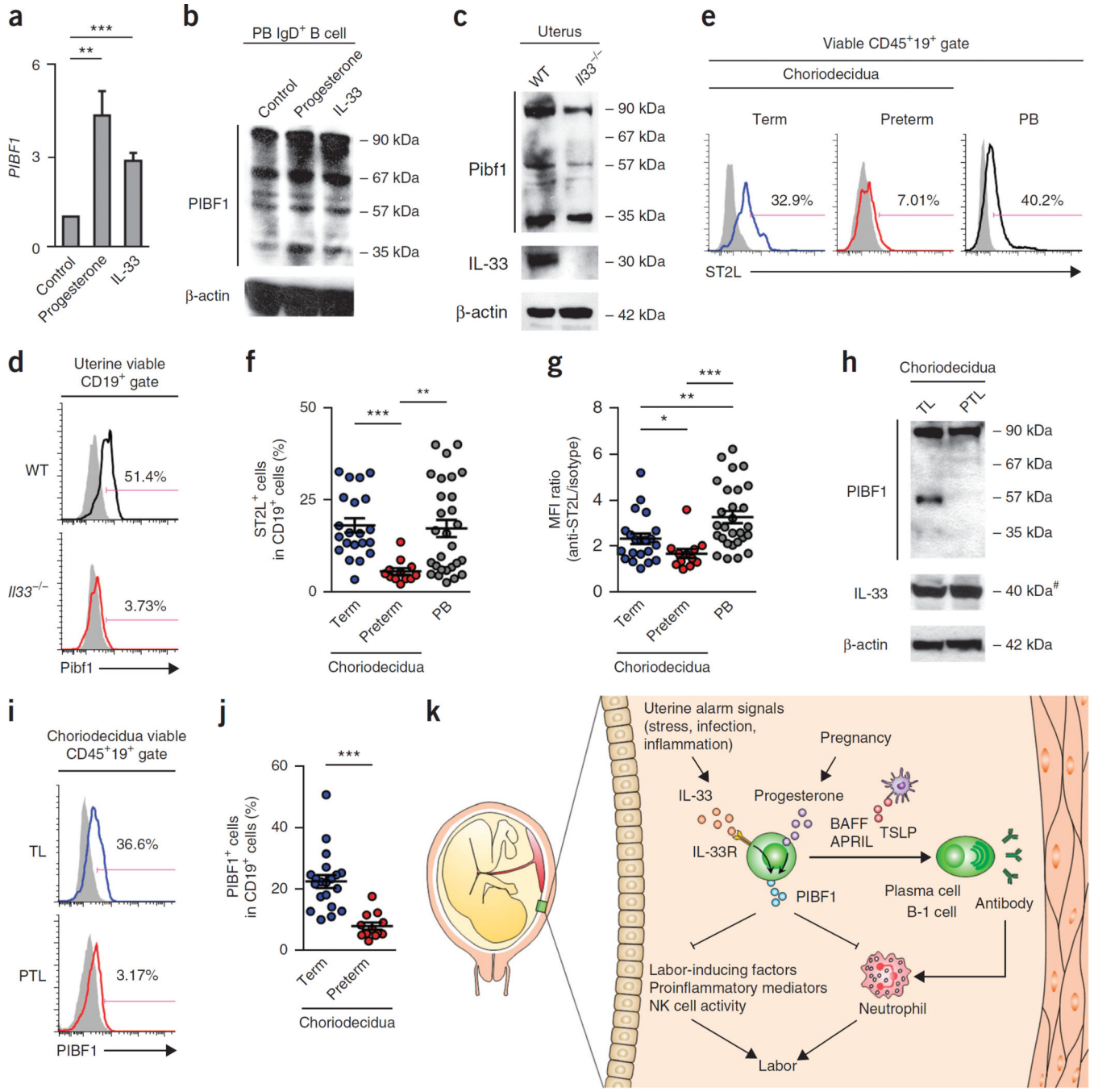

Figure 4.

IL-33-dependent PIBF1 expression by decidual B cells is defective in human PTL. (**a**) Fold change of *PIBF1* transcript in human PB IgD$^+$ B cells after 3 d of stimulation with progesterone or IL-33, relative to unstimulated IgD$^+$ B cells. (**b**) Western blot analysis (n = 4) of PIBF1 in human PB IgD$^+$ B cells after 3 d of treatment with medium (control), progesterone or IL-33. Data in **a** and **b** represent the results of nine donors. (**c,d**) Western blot (n = 3) and flow cytometric analyses of PIBF1 expression in uterine tissue or uterine B cells of age-matched pregnant WT and *Il33*$^{-/-}$ mice on gd 16.5. Data represent three mice

per group. (**e**) Flow cytometry of surface ST2L on B cells in choriodecidual tissues of a woman with TL or a woman with PTL or peripheral blood of a healthy donor. (**f,g**) Frequency of $ST2L^+$ B cells and mean fluorescence intensity (MFI) of surface ST2L staining in choriodecidual B cells of women with TL ($n = 21$) or PTL ($n = 12$) and peripheral blood B cells of healthy donors ($n = 28$). (**h**) Western blot analysis ($n = 3$) of PIBF1 and IL-33 expression in choriodecidual tissue of a subject with TL and a subject with PTL. Data represent four TL and four PTL subjects. Pound sign (#) indicates IL-33 runs at a molecular weight higher than its predicted molecular weight. (**i**) Flow cytometric analysis of PIBF1 expression in choriodecidual $CD19^+$ B cells of a woman with TL and a woman with PTL. (**j**) Frequency of $PIBF1^+$ choriodecidual B cells from TL ($n = 20$) and PTL ($n = 12$) subjects. (**k**) A proposed model of choriodecidual-B-cell-mediated protection against PTL via IL-33-induced expression of PIBF1. B cell migration to choriodecidua in pregnancy may be mediated by signals involving α_4 and β_7 integrins. In response to choriodecidual IL-33, an alarmin that is released following uterine stress, inflammation and infection, choriodecidual B cells produce PIBF1 to suppress premature parturition, likely via the inhibition of the production of labor-inducing factors, natural killer (NK) cell activity, neutrophil infiltration and activation, and the production of proinflammatory mediators[30]. Thus, IL-33, choriodecidual B cells and PIBF1 constitute a protective axis to promote term pregnancy by counteracting uterine stress, inflammation and infection. In PTL, choriodecidual B cells undergo aberrant expansion, increased activation and differentiation into plasma cells or B-1 cells, and secrete antibodies that can trigger labor-inducing inflammatory cascades, such as complement and neutrophil activation. Furthermore, the protective axis involving IL-33, choriodecidual B cells and PIBF1 is defective in PTL, likely as a result of the aberrant downregulation of ST2L on choriodecidual B cells. $*P < 0.05$, $**P < 0.01$, $***P < 0.001$, by two-tailed t test (**a,j**) or two-tailed Mann–Whitney U test (**f,g**).